Optimisation of shimmy suppression device in an aircraft main landing gear

2016 J. Phys.: Conf. Ser. 744 012066

(http://iopscience.iop.org/1742-6596/744/1/012066)

Optimisation of shimmy suppression device in an aircraft main landing gear

Yuan Li[1], **Jason Zheng Jiang**[1] **and Simon Neild**[1]
[1]Department of Mechanical Engineering, University of Bristol, Bristol BS8 1TR, UK
E-mail: yl14470@bristol.ac.uk

Abstract. In earlier publications of landing gear shimmy analysis, efforts have concentrated on predicting the onset of shimmy instability and investigating how to stabilise shimmy-prone landing gears. Less attention has been given to the improvements of shimmy performance for a gear that is free from dynamic instability. This is the main interest of this work. We investigate the effectiveness of a linear passive mechanical device that consists of springs, dampers and inerters on suppressing landing gear shimmy oscillations. A linear model of a Fokker 100 main landing gear and two configurations of candidate shimmy suppression device have been presented. Considering the physical shimmy motions, time-domain optimisation of the parameters in the shimmy suppression devices, using a cost function of maximum amplitude of gear torsional-yaw motion, has been carried out. The performance advantage of a shimmy suppression device incorporating inerter has been presented.

1. Introduction

One of the essential design requirements for aircraft landing gear is that the gear should be free from excessive vibrations and dynamic instabilities, such as shimmy the topic of this paper. The literature indicated that shimmy can occur during aircraft take-off, landing or taxiing and can lead to passenger discomfort, or even in extreme cases disastrous failure of the gear [1]. In order to avoid such undesirable oscillations, various physical solutions are available in modern aircraft, such as the shimmy damper. In [2], it has been shown that a torque link apex shimmy damper can increase the yaw damping to avoid shimmy instability. In landing gear shimmy analysis, most efforts have concentrated on predicting the onset of shimmy instability and investigating how to stabilise shimmy-prone landing gears. Less attention has been given to the improvement of shimmy performance for a gear that is free from dynamic instability, which is the purpose of this work.

The accuracy of landing gear shimmy analysis is dependent on various aspects, such as the mathematical models and analytical methods. Since the elastic tyres play an important role in vehicle shimmy analysis, significant efforts have been made to model the tyre dynamics, including the point contact method proposed by Moreland [3] and the stretched-string tyre model by Von Schlippe and Dietrich [4]. The latter model has been widely accepted in vehicle shimmy analysis and extended by Smiley [5], Segel [6] and Pacejka [7] who provided alternative approximations in the model. Apart from tyre modelling, various analytical methods have been developed and were dependent on the proposed mathematical models. Some linear or quasilinear methods are still used in landing gear shimmy analysis, especially efficient on small amplitude shimmy vibration cases. Such examples can be found in [2, 5, 8]. Since the real landing gear systems

exhibit significant nonlinear characteristics, some researchers studied the landing gear shimmy behaviour using nonlinear dynamics methods [9–11]. Time-domain simulation is also a valuable tool for predicting the dynamics of both linear and nonlinear systems [8].

In the present paper, we investigate the possibility of improving landing gear shimmy performance using a passive device consisting of springs, dampers and inerters. The inerter [12] is defined as a one-port mechanical element with the property that the applied force is proportional to the relative acceleration between two terminals. With introduction of the inerter, a complete analogy between mechanical systems and electrical circuit synthesis can be achieved. Thus, a much wider range of passive suspension structures can be realised mechanically. Performance benefits have been identified for various mechanical and civil systems, including automobile suspensions [13], railway suspensions [14–16] and building suspensions [17]. The inerter has been successfully deployed in Formula One racing since 2005 [18]. The earlier work on the application of inerter to landing gear shimmy can be found in [19]. In [19], Xin et.al. concluded that the application of inerter may destabilise the system if the gear geometry parameters were not chosen appropriately. Furthermore, they also investigated the effects of inerter on the shimmy performance considering different linear landing gear models. This work was expanded by Liu et.al. [20]. They studied the influence of inerter on the responses of the nonlinear and its linearised models under different initial conditions.

This paper is organised as follows. Based on the work presented by Van Der Valk and Pacejka [2], a model of a Fokker 100 main landing gear (MLG) is presented in Section 2, along with two candidate shimmy suppression configurations. In order to determine the effectiveness of shimmy suppression device, time-domain optimisation is carried out in Section 3. Improvement by geometric modifications of main landing gear has been presented as a benchmark. According to the optimisation, beneficial shimmy suppression schemes are proposed. Conclusions have been drawn in Section 4.

2. A main landing gear model and candidate shimmy suppression configurations

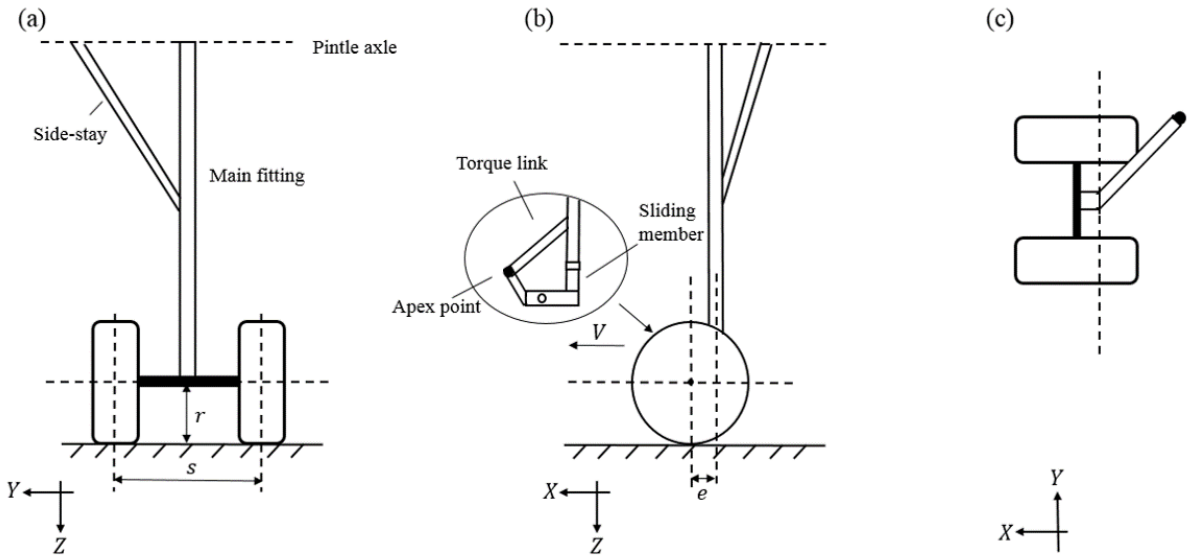

Figure 1. Schematic view of the dual-wheel Fokker 100 MLG geometry. Global coordinates are aligned with X in the forward direction and Z pointing vertically downwards.

In this work, the dynamics of a Fokker 100 MLG is predicted using a mathematical model developed by Van der Valk and Pacejka [2]. The model characterises the motion of the system in terms of several oscillatory degrees of freedom (DOFs) of the MLG and tyre dynamics. Two candidate layouts for the shimmy suppression device are presented, one of which is the conventional shimmy damper configuration while the other one includes an inerter in parallel with the shimmy damper.

2.1. Description of the dynamic system

The Fokker 100 MLG model is illustrated in Figure 1 through different views. The gear structure consists of a main fitting, side-stay, sliding member, and axle assembly, etc. As sketched in Figure 1, a global coordinate frame (XYZ) is defined and its origin is fixed in the pintle axle. X points in the direction of aircraft forward speed V, Z axis vertically downwards, and Y completes the right-handed coordinate system. The two wheels are connected by the wheel axle, with the distance s, which offsets the main fitting axis via a mechanical trail e.

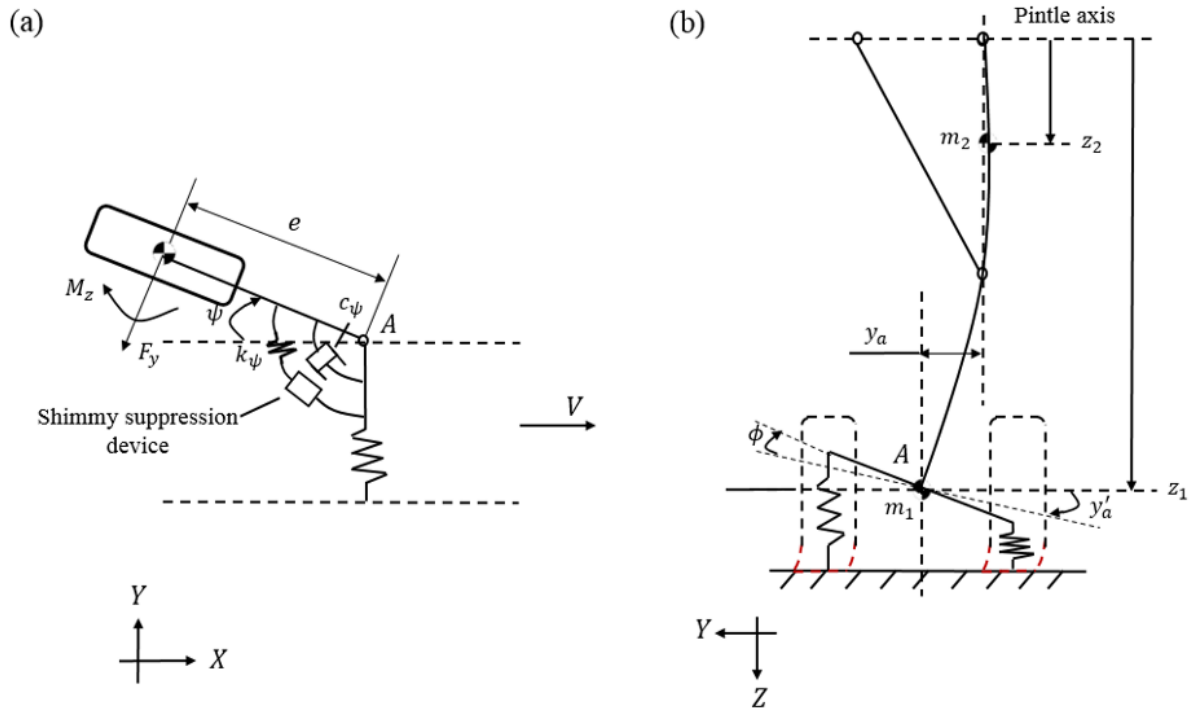

Figure 2. (a) Torsional-yaw ψ DOF, (b) lateral deflection and slope of A y_a, $y_a{}'$ and roll ϕ DOF (a modified version of Figs. 2 and 3 in [2]).

Three important motions are used to characterise the MLG motions: torsional-yaw motion of the sliding member about the center line of the main fitting ψ (positive if clockwise), the lateral bending of the leg y and torsional-roll motion of the wheel axle about the trail ϕ (positive if clockwise). Figure 2 illustrates the sign conventions of these DOFs and the tire lateral deformation. In Fig. 2(a) the two wheels are collapsed into one plane with respect to the point A. Torsional-yaw stiffness and damping (k_ψ, c_ψ), along with torsional-roll stiffness and damping (k_ϕ, c_ϕ), are included due to the effects of the structure itself, the shock strut or the steering mechanism. Note that in this study we use the conventional notifications k for spring and c for damper, different from the ones used in [2] (c for spring and k for damper).

Modal representation is used to indicate the lateral deflection with modal coordinate η and the relationship can be written as

$$y(z,t) = f(z)\eta(t) \tag{1}$$

where $f(z)$ denotes the approximate mode shape belonging to the first mode of the freely hanging landing gear. The landing gear is regarded as a beam with two concentrated masses representing unsprung mass m_1 and the main fitting m_2.

The three oscillatory motions are coupled via the tyre lateral motion. The tyres are assumed to have linear spring characteristics k_v in vertical direction and for its lateral compliance, we would apply the straight tangent tyre model to characterise such lateral motion. In this tyre model, the later displacement v_1 (measured in meters) of leading point of contact edge can be given by

$$v_1 = \sigma\alpha^{'}$$

where σ is defined as the tyre relaxation length and $\alpha^{'}$ the tyre lateral deflection angle. The lateral force F_y due to the tyre deformation and the tyre self-aligning moment M_z are expressed as linear functions of $\alpha^{'}$, giving

$$F_y = C_{F\alpha}\alpha^{'} \tag{2}$$

$$M_z = -C_{M\alpha}\alpha^{'} \tag{3}$$

where $C_{F\alpha}$ and $C_{M\alpha}$ denote tyre restoring force coefficient and aligning moment stiffness respectively. It should be noted that the tyre slip angle is equal to its lateral deformation angle if the MLG is in its undeflected state. To assess the influence of the MLG rolling motion on tyre wear, the variation of tyre pressure is taken into account. Such influence can be identified by a ratio between the variation of tyre pressure ΔF_z and vertical static load F_{z0} on one tyre. The ratio can be written as

$$\Lambda = \frac{\Delta F_z}{F_{z0}} = \frac{\frac{1}{2}k_v s(\phi + y_a{}^{'})}{F_{z0}} \tag{4}$$

where the value of F_{z0} is provided by the experiment conducted in [2].

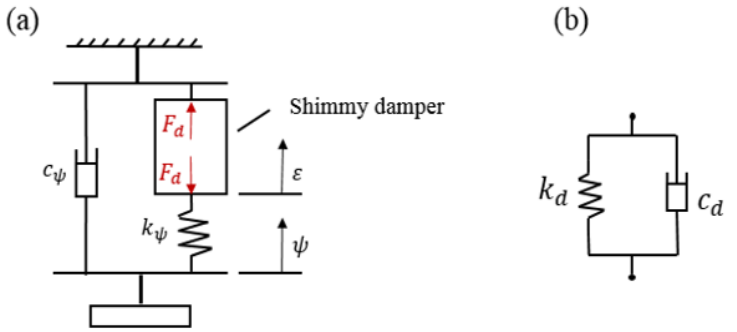

Figure 3. (a) The effective overall torsional-yaw structural stiffness k_ψ, ψ and ε DOFs, (b) the default shimmy damper used in this study inspired by [2].

Of specific interest in our analysis is the effectiveness of the shimmy suppression device, conventionally, a shimmy damper. This device is installed at the torque link apex point (as shown in Figure 1(b)) to provide additional damping to the gear's torsional motion. In the mathematical model, we use a force generated by the shimmy suppression device, F_d, to represent the effects of the device generally, as shown in Figure 3(a). This force could differ from device to

device. For a conventional shimmy damper, its characteristics are translational while using the distance from torque link apex to the centre line of the leg, translational characteristics could be converted into equivalent torsional characteristics about the strut line. Hence in this study, we use the rotational DOF, ε, to represent the motion of shimmy suppression device. Moreover, the default shimmy damper is assumed to consist of a linear rotational damper c_d and spring k_d in parallel and a schematic view is given in Figure 3(b). Thus for the conventional shimmy damper, we have

$$F_d = c_d\dot{\varepsilon} + k_d\varepsilon \tag{5}$$

2.2. Equations of motion

Using Lagrange's equation, we establish the equations of motion which can be written as

$$I_{\psi tot}\ddot{\psi} + m_1 e f_a\ddot{\eta} + c_\psi\dot{\psi} - 2I_{yb}\Omega(f_a{}'\dot{\eta} + \dot{\phi}) + F_d + 2(eC_{F\alpha} + C_{M\alpha})\alpha' = 0 \tag{6}$$

$$(m_f + I_\phi f_a{}'^2)\ddot{\eta} + m_1 e f_a\ddot{\psi} + I_\phi f_a{}'\ddot{\phi} + 2I_{yb}\Omega f_a{}'\dot{\psi} + 2m_f\zeta_n\tau_1\dot{\eta} + \tau_1{}^2 m_f\eta$$
$$+2C_{F\alpha}(f_a + r f_a{}')\alpha' + \frac{1}{2}k_v s^2 f_a{}'(f_a{}'\eta + \phi) = 0 \tag{7}$$

$$I_\phi(\ddot{\phi} + f_a{}'\ddot{\eta}) + 2I_y b\Omega\dot{\psi}) + c_\phi\dot{\phi} + k_\phi\phi + 2rC_{F\alpha}\alpha' + \frac{1}{2}k_v s^2(f_a{}'\eta + \phi) = 0 \tag{8}$$

$$-\sigma\dot{\alpha}' + V(\psi - \alpha') + (f_a + r f_a{}')\dot{\eta} + r\dot{\phi} + (e - a)\dot{\psi} = 0 \tag{9}$$

$$F_d - k_\psi(\psi - \varepsilon) = 0 \tag{10}$$

where $I_{\psi tot}$ is the total torsional-yaw moment of inertia, I_{yb} is the polar moment of inertia of the wheel, tyre and brake, I_ϕ is the torsional-roll moment of inertia, Ω is the tyre rotational velocity and f_a and $f_a{}'$ are the deflection and slope of the lateral mode shape at the bottom of the leg respectively. m_f denotes the modal mass of hanging landing gear while τ_1 its undamped first natural frequency and ζ_n the first relative damping of the lateral mode. σ is the relaxation length of the tyre, with loaded radius r and half the tyre contact length a.

Therefore, we have 5 DOFs in the equations of motion, which are ψ, η, ϕ, α' and ε to model MLG motions. The parameter values for MLG geometry and tyre are taken from [2] and some parameters that were unspecified in [2] but needed in this study are summarised in Table 1. Specifically, the operation case used in this work is that the shock strut deflection is 0.25 m and the forward speed is 50 m/s.

Table 1. Some system parameter values used in the model.

Symbol	Parameter	Value	Units
c_ψ	Torsional-yaw damping values of the gear	1.06×10^3	Nms·rad^{-1}
c_ϕ	Torsional-roll damping values of the gear	540.0	Nms·rad^{-1}
k_v	Tyre spring stiffness in vertical direction	8.64×10^5	N·m^{-1}
k_ψ	Overall torsional-yaw structural stiffness of the gear	6.45×10^5	Nm·rad^{-1}
k_ϕ	Torsional-roll structural stiffness of the gear	2.15×10^6	Nm·rad^{-1}
τ_1	Undamped first natural frequency of hanging landing gear	72.0	Hz
ζ_n	First relative damping of the lateral mode	0.05	-

2.3. Candidate shimmy suppression configurations

In Figure 4, we introduce two candidate layouts for the shimmy suppression device. Both proposed structures will be used to replace the solid box illustrated in Figure 3(a). Layout S1 models the conventional shimmy damper configuration, a parallel spring-damper structure. S2 includes an extra inerter in parallel with S1. Even though the layouts S1 and S2 will not exploit the full possibility of passive suspensions, they are still worth investigating to see whether these relatively simple structures can result in significant benefits.

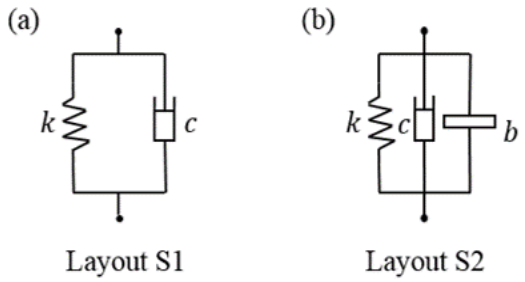

Figure 4. Candidate shimmy suppression configurations.

3. Results for time-domain analysis

In order to identify the effectiveness of candidate shimmy suppression device, time-domain optimisation is performed. We consider an idealised tyre excitation from an uneven runway in the time-domain simulation. MLG torsional-yaw motion is treated as the typical shimmy motion which needs to be controlled via the suppression device and its corresponding peak amplitude and settling time are defined as performance measures in our analysis. With the default shimmy damper setting, the baseline improvement provided only by MLG geometry modifications are identified. Following this, improvement on the peak amplitude of gear torsional-yaw motion can be provided by several beneficial suppressing shimmy schemes. In addition, the tyre responses provided by the beneficial schemes are investigated. For all the optimisations carried out in the present paper, we used the Matlab command `patternsearch`, which is to find the minimum of a function. This solver does not require the gradient of the problem and is beneficial for the time-domain simulation in our study. Then the command `fminsearch` was used for fine-tuning of the parameters.

3.1. Initial operation conditions

A typical situation in which the tyres are disturbed by unevenness of the runway, leading to initial excitations applied to the tyres, is considered. We assume the tyre travel direction is disturbed suddenly, causing the corresponding initial input to the tyre slip angle α. As presented in Section 2, we apply the $\alpha(t=0) = \alpha^{'}(t=0) = 0.1$rad as the initial excitation to the system. It should be noted that except for the excitation, all the other states should have zero initial values. In addition, the system is assumed to operate under a constant forward velocity ($V = 50$m/s) and the involved parameter values always keep constant as the default setting.

3.2. Time-domain performance measures

In the analysis of landing gear shimmy problem, the torsional-yaw motion plays a significant role in terms of the gear fatigue life [21]. Other influences, like the tyre lateral deformation and the coupling MLG roll motion that deforms the tyre vertically, results in tyre wear and further affect the MLG performance. For the coupling roll effects on tyre pressure, the ratio Λ (as defined in Section 2) is treated as a measure to identify such impact. Applying the initial

tyre excitation, the time history of Λ can be obtained. The motion is heavily damped with the maximum Λ of 17.53%. However, even if we improve the coupling MLG roll motion $(\phi + y_a{}')$, only a limited improvement could be obtained on the ratio Λ. Hence we don't regard such coupling effects as the performance that needs to be improved. However, since the tyre motion plays an importance role in tyre-ground contact dynamics, tyre lateral motion is still of specific interest to be investigated. Therefore, we investigate the effectiveness of an inerter-combined suppressing shimmy device on the torsional-yaw motion and we still keep an eye on how the tyre lateral motion is affected.

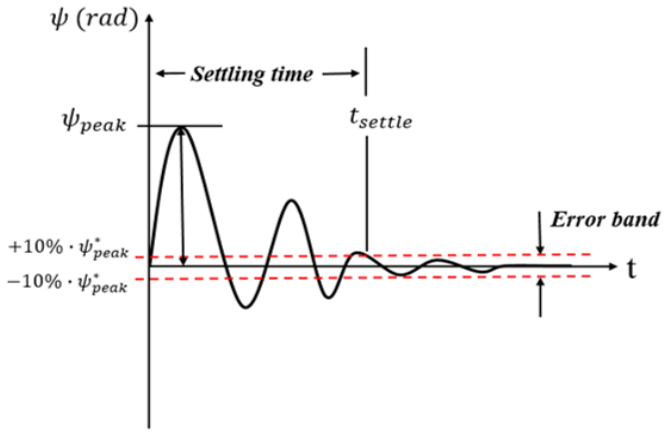

Figure 5. The definitions of two performance measures used in time-domain optimisation over torsional-yaw motion.

Specifically, the performance measures are defined as the peak magnitude ψ_{peak} and settling time t_{settle} of torsional-yaw motion. The peak magnitude ψ_{peak} is defined by the maximum value of torsional-yaw response during a certain timespan 0.5 s. Different from the traditional definition, t_{settle} is the time elapsed from 0 to the time at which the response has entered and remained within a specified error band. In general, the boundary of this error band is 1/3 of the original amplitude [22]. To achieve better performances and compare with the default shimmy damper, the error band here is defined more strictly as $\pm 10\%$ of ${\psi_{peak}}^*$ as shown in Figure 5. ${\psi_{peak}}^*$ is the nominal peak amplitude produced by the system with the default shimmy damper. Since there could be a trade-off between the two performance measures in general, in the optimisation ψ_{peak} will be used as a cost function while a maximum on t_{settle} must be satisfied.

3.3. Baseline improvement by geometric modifications

From the conclusions of the preceding analysis, certain MLG features, including gear geometry, gear structural parameters and tyre characteristics, play an important role in stabilising shimmy-prone gears. The modifications of the later two aspects are hard to control comparing with the geometry thus these parameters remain constant in this analysis. We consider two key MLG geometry parameters, wheel distance and mechanical trail, as the design variables. The improvement provided by the geometric modifications on the cost function, ψ_{peak}, is treated as a benchmark for the following optimisation of shimmy suppression device. Note that the default setting for the shimmy suppression device is used at this stage. Wheel distance s and mechanical trail e are varied in terms of scaling coefficient t^* where ${t_s}^*$ and ${t_e}^*$ are for the two cases respectively. Both parameters represented by ${t_s}^*$ and ${t_e}^*$ have been normalised with

respect to nominal values, e.g.

$$t_s{}^* = \frac{s^{'}}{s_{nom}}$$

where $s^{'}$ denotes the modified wheel distance and s_{nom} the nominal value.

To help understand what is happening in physical motions (typically torsional-yaw motion) when varying the wheel distance, the transient responses are plotted in Figure 6. It is observed that the involved responses are varying slightly when $t_s{}^*$ is varied, which is not the case for the system when no shimmy damper is present. We see that decreasing wheel distance could result in smaller magnitudes of torsional-yaw motion and the response decays more quickly, but the effect is small. For $t_s{}^* = 0.5$, the percentage improvement are 3.33% on ψ_{peak}. For the case with varied $t_e{}^*$, it can be checked that the variation of $t_e{}^*$ influence the MLG torsional-yaw motion more significantly comparing with the wheel distance case. But similarly, a reduction of $t_e{}^*$ could lead to the improvement on ψ_{peak} of up to 14.0%.

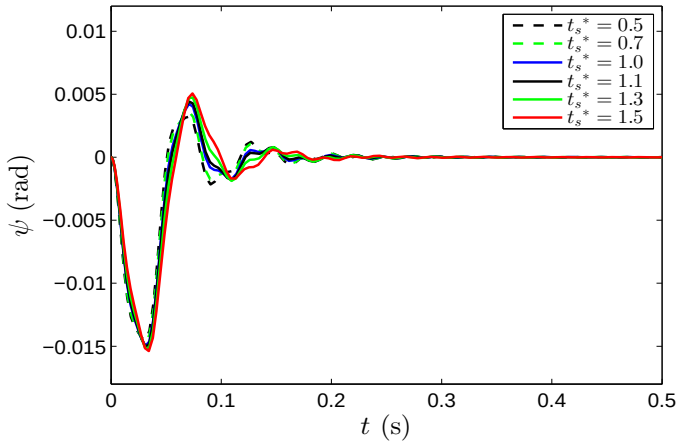

Figure 6. Comparison of ψ time histories when varying $t_s{}^*$ for the system with a default shimmy damper configuration.

3.4. Optimisation of proposed shimmy suppression configurations

The time-domain optimisation is carried out using the cost function ψ_{peak} while ensuring that t_{settle} will not be worse than the default setting. Both the candidate layouts will be optimised. Applying the initial input to the simulation, the ψ_{peak} and t_{settle} of the default landing gear equal to 0.015rad and 0.110s respectively. So we set $t_{settle} \leq 0.110$s as a constraint.

Table 2. Summary of optimisation results.

Layouts	ψ_{peak} (rad)	t_{settle} (s)	Impro. (%)	Parameter values (Nm·rad^{-1}, Nms·rad^{-1}, Nms^2·rad^{-1})
Default	0.015	0.110	-	$k = 1.85 \times 10^5, c = 7.40 \times 10^3$
$S1$	0.0125	0.105	12.67	$k = 1.11 \times 10^5, c = 1.44 \times 10^4$
$S2$	0.0108	0.096	28.0	$k = 2.90 \times 10^6, c = 1.50 \times 10^4, b = 318.71$

The optimisation results are summarised in Table 2 and related responses are illustrated in Figure 7. Rows 2 - 3 of Table 2 gives the beneficial schemes which improve ψ_{peak}. It can be seen that Layout S1 provides a 16.67% improvement on ψ_{peak} over the default shimmy damper scheme. With the introduction of an inerter, the percentage improvement achieved by S2 increased to 28.0% in comparison with the conventional layout. The error band as we defined has been presented in two black lines in Figure 7, which shows the restrictions on settling time are always satisfied for the two beneficial schemes.

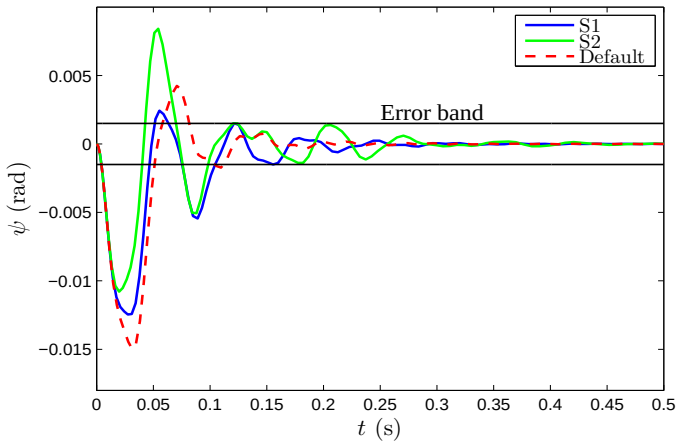

Figure 7. Comparison of ψ time histories for the default and beneficial schemes.

Even though we obtained up to 28.0% of improvement on ψ_{peak} from the optimisation, it can be noticed from Figure 7 that the second peak amplitudes of the responses are increased for both beneficial schemes, especially for S2. Thus, to further improve torsional-yaw motion, an extra restriction on the second peak amplitude has been included, together with the restriction on t_{settle}. In the optimisation with the restriction on the second peak, we use the superscript † to denote. Rows 2 - 3 of Table 3 gives the optimal solutions which improve ψ_{peak} and limit the values of second peaks. The improved responses are illustrated in Figure 8. It can be observed that the second peak amplitudes are decreased significantly compared with Figure 7. The trade-off between ψ_{peak} and the second peak amplitude leads to relatively smaller improvement in the cost function, ψ_{peak}. However, the improvement, 16.67% for $S1^{\dagger}$ and 26.67% for $S2^{\dagger}$, is still considerable. Hence, we propose $S2^{\dagger}$ as the most beneficial scheme for suppressing the MLG shimmy here.

Table 3. Summary of optimisation results reducing the second peaks.

Layouts	ψ_{peak} (rad)	t_{settle} (s)	Impro. (%)	Parameter values ($Nm{\cdot}rad^{-1}$, $Nms{\cdot}rad^{-1}$, $Nms^2{\cdot}rad^{-1}$)
Default	0.015	0.110	-	$k = 1.85 \times 10^5, c = 7.40 \times 10^3$
$S1^{\dagger}$	0.0131	0.101	16.67	$k = 1.43 \times 10^5, c = 1.18 \times 10^4$
$S2^{\dagger}$	0.0110	0.104	26.67	$k = 7.16 \times 10^5, c = 1.30 \times 10^4, b = 144.85$

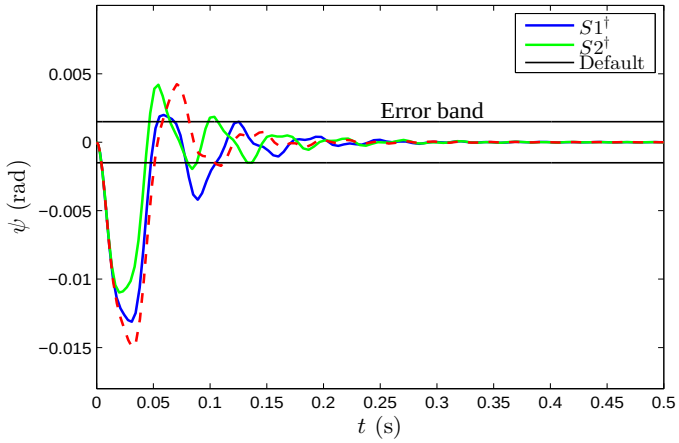

Figure 8. Comparison of ψ time histories with the restriction of the second peaks for the default and beneficial schemes.

3.5. Tyre lateral motion

As mentioned in the Section 3.2, tyre lateral motion, v_1 (instead of $\alpha^{'}$ DOF), is the motion which reflects the tyre-ground contact dynamics and influence the aircraft ground manoeuvre significantly. Hence we will further check the tyre lateral responses achieved by beneficial schemes. Figure 9 illustrates the comparison plots of tyre lateral motions between the default and two beneficial shimmy suppression device schemes, $S1^{\dagger}$ and $S2^{\dagger}$. It can be observed that the responses are quite similar since tyre lateral motion appears to be relatively decoupled with torsional-yaw motion here. This indicates that tyre motion will not become worse when implementing the shimmy suppression device, that is beneficial to the torsional-yaw motion, into the original system.

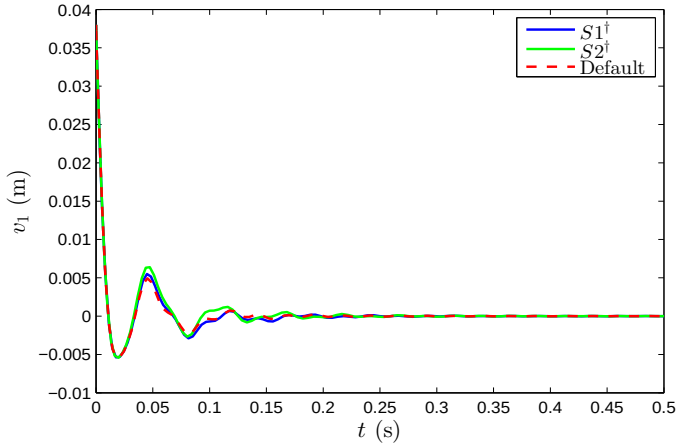

Figure 9. Comparison of tyre lateral motions (v_1) for the default shimmy damper, $S1^{\dagger}$ and $S2^{\dagger}$.

4. Conclusions

The main focus of this study is to investigate the potential benefits of the shimmy suppression device incorporating inerter on a Fokker 100 MLG. We present a five DOFs ordinary differential equation model. Based on this model, a time-domain optimisation is carried out and is of primary interest in this study. We consider a typical initial operation condition for the system

and torsional-yaw motion is chosen as the key shimmy performance that needs to be controlled here. Using the cost function of the peak amplitude of torsional-yaw motion, we perform the optimisation over two candidate shimmy suppression configurations. Separate from the stability problem, modifying the landing gear geometry, specifically the wheel distance and mechanical trail, appears to be able to improve the landing gear torsional-yaw motion slightly. Considering the improvement on the peak amplitude (26.67%) with a restriction on the settling time and the second peak of the response, a parallel inerter-spring-damper scheme is proposed as the beneficial configuration for Fokker 100 main landing gear shimmy suppression. However, although the benefits of the proposed inerter-combined device are identified through the optimisation, it is still not clear why the inclusion of inerter can help suppress shimmy oscillations more effectively. Thus, to investigate the exact reasons would be the direction of our future work.

Acknowledgments
The authors would like to acknowledge the support of the EPSRC and the China Scholarship Council: Simon Neild is supported by an EPSRC fellowship EP/K005375/1 and Yuan Li is supported by a China Scholarship Council studentship.

References

[1] Glaser J and Hrycko G 1995 *81st Meeting of the AGARD Structures and Materials Panel* (DTIC Document)
[2] Van der Valk R and Pacejka H 1993 *Vehicle system dynamics* **22** 97–121
[3] Moreland W J 1954 *Journal of the Aeronautical Sciences (Institute of the Aeronautical Sciences)* **21**
[4] Von Schlippe B and Dietrich R 1947 *NACA TM* **1365**
[5] Smiley R F 1957 *NACA* **1299**
[6] Segel L 1966 *Journal of Manufacturing Science and Engineering* **88** 37–44
[7] Pacejka H B 1965 *Proc. of the Institution of Mechanical Engineers: Automobile Division* **180** 251–268
[8] Somieski G 1997 *Aerospace Science and Technology* **1** 545–555
[9] Woerner P and Noel O 1995 *81st Meeting of the AGARD Structures and Materials Panel* (DTIC Document)
[10] Gordon J T and Merchant H E 1978 *Journal of Aircraft* **15** 155–159
[11] Li G 1993 Modelling and analysis of a dual-wheel nosegear: shimmy instability and impact motions Tech. rep. SAE Technical Paper
[12] Smith M C 2002 *Automatic Control, IEEE Transactions* **47** 1648–1662
[13] Smith M C and Wang F C 2004 *Vehicle System Dynamics* **42** 235–257
[14] Jiang J Z, Matamoros-Sanchez A Z, Goodall R M and Smith M C 2012 *Vehicle System Dynamics* **50** 263–276
[15] Wang F C and Liao M K 2010 *Vehicle System Dynamics* **48** 619–643
[16] Jiang Z, Matamoros-Sanchez A Z, Zolotas A, Goodall R and Smith M 2013 *Proceedings of the Institution of Mechanical Engineers, Part F: Journal of Rail and Rapid Transit* 0954409713511592
[17] Lazar I, Neild S and Wagg D 2014 *Earthquake Engineering & Structural Dynamics* **43** 1129–1147
[18] 2008 Cambridge university engineering department news item URL `http://www.eng.cam.ac.uk/news/stories/2008/McLaren/`

[19] Xin D, Yuance L and Chen M Z 2015 *Control Conference (CCC), 2015 34th Chinese* (IEEE) pp 2066–2071

[20] Liu Y, Chen M Z and Tian Y 2015 *Information and Automation, 2015 IEEE International Conference on* (IEEE) pp 696–701

[21] Krüger W, Besselink I, Cowling D, Doan D, Kortüm W and Krabacher W 1997 *Vehicle System Dynamics* **28** 119–158

[22] *SAE AIR* **4894**